SCIENTIFIC JOURNAL
EARTH'S CRYOSPHERE

Earth's Cryosphere, 2016, vol. XX, No. 2, pp. 14–22 **http://earthcryosphere.ru/**

REGIONAL PROBLEMS OF EARTH'S CRYOLOGY

COMPARATIVE ANALYSIS OF THE ISOTOPIC COMPOSITION OF ICE WEDGES AND TEXTURE ICES AT THE LAPTEV SEA COAST

A.Yu. Dereviagin, A.B. Chizhov, H. Meyer*, T. Opel*

Lomonosov Moscow State University, Department of Geology,
1, Leninskie Gory, Moscow, 119991, Russia; dereviag@gmail.com
**Alfred Wegener Institute for Polar and Marine Research, 14473, Potsdam, Telegrafenberg A43, Germany*

On the basis of large-scale sampling of syngenetic ice wedges and texture ices at Laptev Sea coast the differences of their isotopic composition ($\delta^{18}O$, δD) throughout the past 50 ka have been analyzed. The transformation of isotopic composition in the contact zone between ice wedges and texture ice has been considered. The analysis of ^{14}C-dated samples demonstrated that the isotopic composition ($\delta^{18}O$, δD) both of ice wedges and texture ices reacts similarly to the well-pronounced paleoclimatic events.

Ice-wedges, texture ices, isotopic analysis, radiocarbon dating, Late Pleistocene, Holocene

INTRODUCTION

Until recently, the pool of data on the isotopic composition of ground ice was hugely dominated by the results of oxygen and hydrogen isotope ($\delta^{18}O$, δD) analysis of ice wedges as a possible source for information on winter paleotemperatures [*Mackay, 1983; Vaikmae, 1989; Vasil'chuk, 1992; Meyer et al., 2002a*]. The extensive database collected during the works of the Russian-German expedition over the period of 1998–2012 in the Laptev Sea coastal region (Fig. 1) included data not only on the isotopic composition of ice wedges (IW) but on texture ices (TI) in the surrounding frozen sediments containing ice veins. The section of Late Pleistocene – Holocene deposits with ground ice of both types comprehended by the research has been studied to a depth of 30–40 m in the age range of 40–50 ka. The obtained data were used in the comparative analysis of the isotopic composition of two, the most widespread types of ground ice – ice wedges and texture ices – that form ice-rich permafrost strata of the Arctic lowlands at the Laptev Sea coast. The analysis expediency is substantiated by recent advancements in the permafrost isotopic geocryology and objectives of this study aiming to investigate paleogeographic conditions for the formation of ground ices and to determine their genesis.

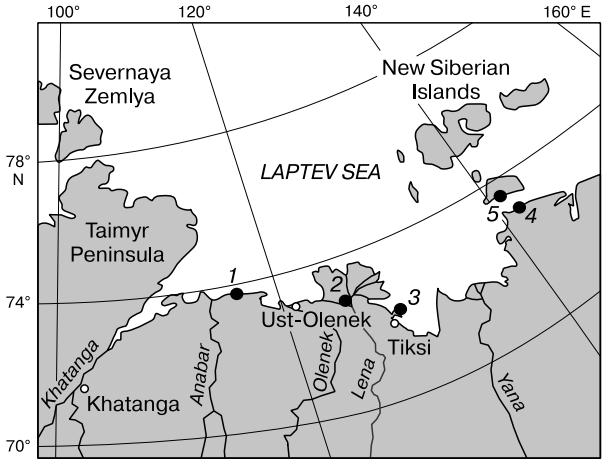

Fig. 1. Location of sites.

1 – Cape Mamontov Klyk; *2* – Lena Delta; *3* – Bykovsky Peninsula; *4* – Oygossky Yar Coast; *5* – Bolshoy Lyakhovsky Island.

STUDY AREA

The study area covers the coastal lowlands of the Laptev Sea from the Kondratieva Rv. (Oigossky Yar) in the east, extending as far as the Anabar Rv. in the west (Cape Mamontov Klyk area). We used the data on radiocarbon (^{14}C) dating of organic residues in the surrounding sediments and ice wedges, the isotopic composition of ground ice in the outcrops on the following sites: Cape Mamontov Klyk Peninsula Bykovsky, Lena Delta, Oygossky Yar coast, Bolshoi Lyakhovsky (Fig. 1). The upper parts of the section within these sites are represented by deposits of Late Pleistocene (Karginsky and Sartan periods) and Holocene age. The sections are composed mostly of Ice Complex deposits. Their cryogenic texture is discussed in detail in the previously published studies [*Meyer et al., 2002a,b; Schirrmeister et al., 2008, 2011; Dereviagin et al., 2013*].

The severe Arctic climate of the study region is characterized by long cold winters and notably short rainy summers. The mean annual air temperature according to the weather station records ranges from −13.0 to −15.7 °C. Region-wide averages of annual precipitation constitute 230–300 mm in the west and in the central part, decreasing to 140–180 mm in the east. Of these, up to 70 % fall mostly as rain during the summer. The snow cover is established by the end of September and degrades late in June. The snow cover depth generally is not more than 20–30 cm. The area is located in the zone of continuous permafrost, with thickness of 400–600 m [*Yershov, 1989*]. The mean annual temperature of sediments is about −12 °C. Thickness of the active layer (ALT) does not exceed 0.5 m.

RESULTS AND DESCUSSION

The isotopic analysis of 1553 ice cores from ice wedges and 222 texture ice samples was conducted at the Wegener Institute for Polar and Marine Research (Potsdam, Germany). The analysis results are expressed per mille (‰) relative to the standard mean ocean water (SMOW). The measurement error is <0.1 ‰ for $\delta^{18}O$ and <0.8 ‰ for δD. The ^{14}C dating of organic remains was carried out by AMS-Lab method at the Laboratory for Radiometric Dating and Stable Isotope Research, the Leibniz University of Kiel (Germany).

The results of the exposed ground ice sampling are usually represented in the form of the $\delta^{18}O$ (δD)-diagram reflecting their variations with depth. Given that the sample of ices (TI and IW) from the same level may differ in age by several thousand years, as well as climatic and landscape conditions of their isotopic composition formation, using a diagram for comparison of the isotopic composition of TI and IW would not therefore be quite appropriate. This is evidenced by numerous data from detailed sampling along horizontal profiles of syngenetic ice wedges 3–5 meters in width, showing the $\delta^{18}O$ amplitude oscillation reaching 3–4 ‰ [*Meyer et al., 2002a,b; Derevia-gin et al., 2010*].

Approximate ages of TI and IW in the syncryogenic sequences were determined by the radiocarbon dating of organic microinclusions. However, there exists critical limitations in comparing samples of IW and TI with similar absolute ages, which is primarily associated with very rare finds of organic material sufficient for accelerator mass spectrometry AMS-dating of ice cores from ice wedges. The error of the ^{14}C-method determined at the laboratory for each sample as a $\pm\Delta t$ years can also be significant.

The available data (Table 1, *a*, *b*) allowed selecting nine pairs* of dated TI/IW samples with relatively close radiocarbon ages: 1/1, 2/7, 3/8, 6/12, 7/13, 8/14, 9/18, 24/20, 27/22, with difference in ages ranging between 100 and 300 years for the compared samples. Comparisons of TI and IW samples with close radiocarbon ages revealed that in seven out of nine cases, the isotopic composition of TI was heavier than that of IW, while differences between $\delta^{18}O$ values for TI and ice wedges ranged from 0.5 to 7.3 ‰. Only in two cases, TI samples were isotopically lighter than IW: by 0.8 ‰ (pair 9/18) and 0.5 ‰ (pair 2/7). Analysis of the isotopic composition of TI and IW from mass sampling for basic stratigraphic horizons (Table 2, 3) have proven most informative at this stage of the research. Statistical analysis of the isotopic composition data shows that average $\delta^{18}O$ (δD) values for TI in all stratigraphic subunits are generally isotopically heavier those for IW.

This can be explained by the dominance of isotopically lighter snow meltwater in ice wedges, while isotopically heavier rain waters prevail in texture ices. In modern solid precipitation (analyzed location: vicinities of Tiksi settlement), average concentration of ^{18}O has dramatically decreased to −31.5 ‰, and down to −17.1 ‰ in summer precipitation, with the annual value averaging −24.9 ‰. The difference (Δ) between averaged $\delta^{18}O$ values for winter and summer precipitation constitutes 14.4 ‰.

The difference in isotope concentrations between TI and IW is greatly reduced due to the mixing melt- and rainwaters and at the expense of isotope fractionation. Our research has shown that $\Delta\delta^{18}O$ for modern (younger than 100 years) TI and IW averages 2.8 ‰.

Difference (Δ) between average values of the isotopic composition ($\delta^{18}O$) for TI and for IW varies depending on their age (Table 2). Maximum $\Delta\delta^{18}O$ values are inherent in ices of the Holocene and Karginsky age: 5.4 and 4.2 ‰, respectively. At the end of the Late Pleistocene (Sartan period), this difference tend to be reduced to 3.0 ‰. This is probably due to the change in balance between snowmelt and rain water in their feeding the ground ice. Small Δ values attributed to Sartan time could be due to the dry summers, when melting snow patches were the main source of moisture. High Δ values for Karginsky time may indicate a rapid melting of the snow cover and increased contribution from rainwater to the formation of TI. At this, $\delta^{18}O$ (δD) values for TI and IW (Table 2) indicate that ground ice formation both in Sartan and Karginsky time occurred under very cold climate with low winter air temperatures and mean annual air temperatures.

The difference in average concentrations of ($\delta^{18}O$) isotopes between TI and IW reaches maximum values from the beginning of the Holocene war-

* The value of numerator indicate numbering of TI samples (Table 1, *a*), the denominator indicates numbering of IW samples (Table 1, *b*).

Table 1. **Oxygen-isotope composition of ^{14}C-dated samples from texture ice (*a*) and ice wedges (*b*)***

No.	^{14}C age, years	Error (±), years	$\delta^{18}O$, ‰	No.	^{14}C age, years	Error (±), years	$\delta^{18}O$, ‰
a. Dated texture ices				*b*. Dated ice wedges			
1	300	0	–21.4	1	<100	0	–21.9
2	2785	30	–25.8	2	416	31	–24.2
3	3325	35	–17.5	3	1100	25	–25.4
4	8230	50	–17.7	4	1870	35	–24.9
5	8335	45	–17.1	5	2201	44	–23.6
6	9480	40	–19.9	6	2425	30	–24.6
7	11 060	45	–19.5	7	2623	28	–25.3
8	12 525	50	–25.9	8	3630	84	–24.8
9	14 545	50	–25.9	9	4107	41	–26.0
10	16 350	90	–28.3	10	5178	33	–25.9
11	16 510	60	–28.2	11	6336	44	–25.8
12	17 700	70/40	–29.1	12	9390	60	–27.1
13	18 560	100	–27.5	13	11 180	100	–27.6
14	18 920	70	–28.0	14	12 520	70	–30.5
15	19 500	220/210	–29.2	15	13 060	70	–27.2
16	20 180	80	–28.5	16	13 150	50	–27.3
17	20 600	210/200	–28.0	17	14 200	70	–24.9
18	21 890	90	–29.5	18	14 535	60/55	–25.1
19	24 150	120	–29.3	19	26 050	190	–31.3
20	24 600	170/160	–27.7	20	34 210	740/680	–31.1
21	31 250	1080/950	–26.4	21	37 810	680/630	–23.4
22	33 450	260/250	–25.5	22	40 720	1710/1410	–30.5
23	33 580	240/230	–25.8	23	41 990	1050/930	–30.4
24	34 630	420/400	–29.8				
25	36 020	450/420	–25.9				
26	38 600	930/830	–26.9				
27	40 850	1750/1440	–33.1				
28	43 620	1700/1400	–26.5				
29	45 300	1200/1050	–24.6				
30	47 900	1630/1360	–28.3				

* Radiocarbon dating data were used from [*Andreev et al., 2002; Meyer et al., 2002a,b, 2015; Schirrmeister et al., 2008, 2011; Opel et al., 2011*] supplemented with new data.

Table 2. **Isotopic composition ($\delta^{18}O$, δD) of ground ices (GI): texture ice (TI) and ice wedges (IW) of the Late Pleistocene (Karginsky and Sartan time), Holocene and contemporary time**

Age GI, ka	GI type	*n*	$\delta^{18}O$, ‰			δD, ‰			*A*, ‰	Δ, ‰
			Ave.	Min.	Max.	Ave.	Min.	Max.		
55–25 (Karginsky)	TI	78	–26.2	–34.5	–19.2	–205.2	–254.1	–156.5	15.3	4.2
	IW	598	–30.4	–34.9	–23.9	–237.9	–272.2	–180.6	11.0	
25–10 (Sartan)	TI	61	–27.4	–31.6	–20.0	–208.0	–242.1	–151.5	11.6	3.0
	IW	275	–30.4	–38.0	–25.3	–237.9	–296.0	–191.5	12.7	
<10 (Holocene)	TI	61	–19.9	–28.2	–14.1	–151.6	–204.5	–118.4	14.1	5.4
	IW	616	–25.3	–29.9	–19.2	–192.2	–223.2	–149.2	10.7	
<0.1 (contemporary)	TI	22	–19.4	–23.4	–16.2	–147.1	–178.3	–124.2	7.4	2.8
	IW	64	–22.2	–26.5	–17.9	–169.0	–202.0	–132.3	8.6	

Note. *A* is range of $\delta^{18}O$ (max.–min.); Δ is difference between average $\delta^{18}O$ values of TI and $\delta^{18}O$ WI; *n* is quantity of samples.

Table 3. **Parameters of isotopic composition of ground ices (GI) comprising: texture ices (TI) and ice wedges (IW) of the Late Pleistocene (Karginsky and Sartan time), Holocene and contemporary time**

Age GI, ka	GI type	*n*	d_{exc}, ‰			*a*	*b*	R^2
			Ave.	Min.	Max.			
55–25 (Karginsky)	TI	78	4.7	−10.8	25.8	6.2	−42.4	0.94
	IW	598	5.5	−4.4	15.4	8.3	14.5	0.98
25–10 (Sartan)	TI	61	11.0	−4.4	24.2	7.7	1.8	0.92
	IW	275	5.1	−0.8	10.8	8.2	10.1	0.99
<10 (Holocene)	TI	61	7.4	−5.9	21.4	6.2	−28.7	0.94
	IW	616	10.1	2.9	18.0	7.0	−14.2	0.98
<0.1 (contemporary)	TI	22	8.4	1.0	16.3	7.3	−6.0	0.95
	IW	64	8.5	3.3	13.7	7.3	−6.7	0.97

Note. Deuterium excess (d_{exc}); regression equation coefficients: *a* is slope coefficient, *b* is intercept, R^2 is correlation coefficient; *n* is quantity of samples.

ming and equals – 5.4 ‰. In the Holocene, average winter temperatures increased by approximately 5 °C [*Dereviagin et al., 2010*], while high Δ values suggest that once winters have become warmer, this echoed in the increased duration of summer period and its humidity.

The above data on the concentrations of ($\delta^{18}O$) isotopes and their difference between TI and IW (Δ) are averaged for notably long periods: from ten thousand years to several tens of thousands of years. For shorter periods of time, these characteristics may vary under the influence of changing climate and landscape conditions, hydrological regime, geological processes. In this context, the comparison of the isotopic composition averages for Holocene ices versus modern TI and IW formed during the last 100 years provides spectacular evidence.

The difference in mean isotope concentrations between contemporary TI and IW ($\Delta\delta^{18}O$ = 2.8 ‰) appears considerably lower than in Holocene ices ($\Delta\delta^{18}O$ = 5.4 ‰), which is associated with increased concentration of heavy isotopes in modern ice wedges (Table 2) caused by the increased mean winter air temperature [*Dereviagin et al., 2011*].

The minimum and maximum concentrations of oxygen isotopes ($\delta^{18}O$) with their values as given in Table 2, allowed us to estimate the range of fluctuations in *A* (difference between maximal and minimal values) in IW and in TI. For Holocene and Late Pleistocene syngenetic permafrost sequences with thick ice wedges and well-pronounced schlieren cryogenic textures, the spread of $\delta^{18}O$ values for TI is greater than in Holocene ice wedges (3.4 ‰) and Karginsky period (4.3 ‰).

In Sartan period, the oscillation range of A in ice wedges is 1.1 ‰ higher than in texture ices. More uniform isotopic composition of IW compared to TI (during Karginsky time and the beginning of Holocene) is attributed to the genesis and formation conditions for ice, and by minor impact from the processes of isotope fractionation. In Sartan period, the range of $\delta^{18}O$ values for ice wedges increased at the expense of extremely low values (to –38 ‰), indicating very cold winters featured as unparalleled during the Karginsky period, judging from the data available [*Wetterich et al., 2011*]. At the same time, a relatively low range of values for TI (11.6 ‰) probably indicates dry and cool summer conditions under which the isotopic composition of TI was formed.

In recent growth of ice wedges and in texture ices at the base of AL, the range of $\delta^{18}O$ in TI (7.4 ‰) is to some extent less than in ice wedges (8.6 ‰). Notably, given that formation of modern ground ice is still proceeding, these data can not be considered as final. Homogenization of the isotopic composition of modern TI is favored by the intensely ongoing moisture exchange between the upper layer of permafrost (permafrost table) and active layer during seasonal thawing.

Hydrogen – oxygen isotopes relationship ($\delta D/\delta^{18}O$) in texture ices and ice wedges

In research reports, the isotopic composition ($\delta^{18}O$, δD) of natural water and ice test results are usually represented as δD–$\delta^{18}O$ diagrams and compared with the global meteoric water line (GMWL). This line is described by the regression equation for the mean δD and $\delta^{18}O$ values of precipitation using the weather stations global network data: $\delta D = 8\delta^{18}O + 10$ [*Dansgaard, 1964*]. A deviation measure for the isotopic composition of sample from the GMWL line is determined by the deuterium excess (d_{exc}): $d_{exc} = \delta D - 8\delta^{18}O$. For the GMWL points, d_{exc} = 10 ‰. Samples with d_{exc} greater than 10 ‰ are located on the δD–$\delta^{18}O$-diagram above GMWL, and those with d_{exc} less than 10 ‰ – below it.

Fig. 2 shows δD–$\delta^{18}O$-diagrams for Late Pleistocene (Karginsky and Sartan time), Holocene and modern ice wedges and texture ice (Fig. 2, *a–c* and *d,* respectively). As can be seen from the diagrams, the points corresponding to the isotopic composition of

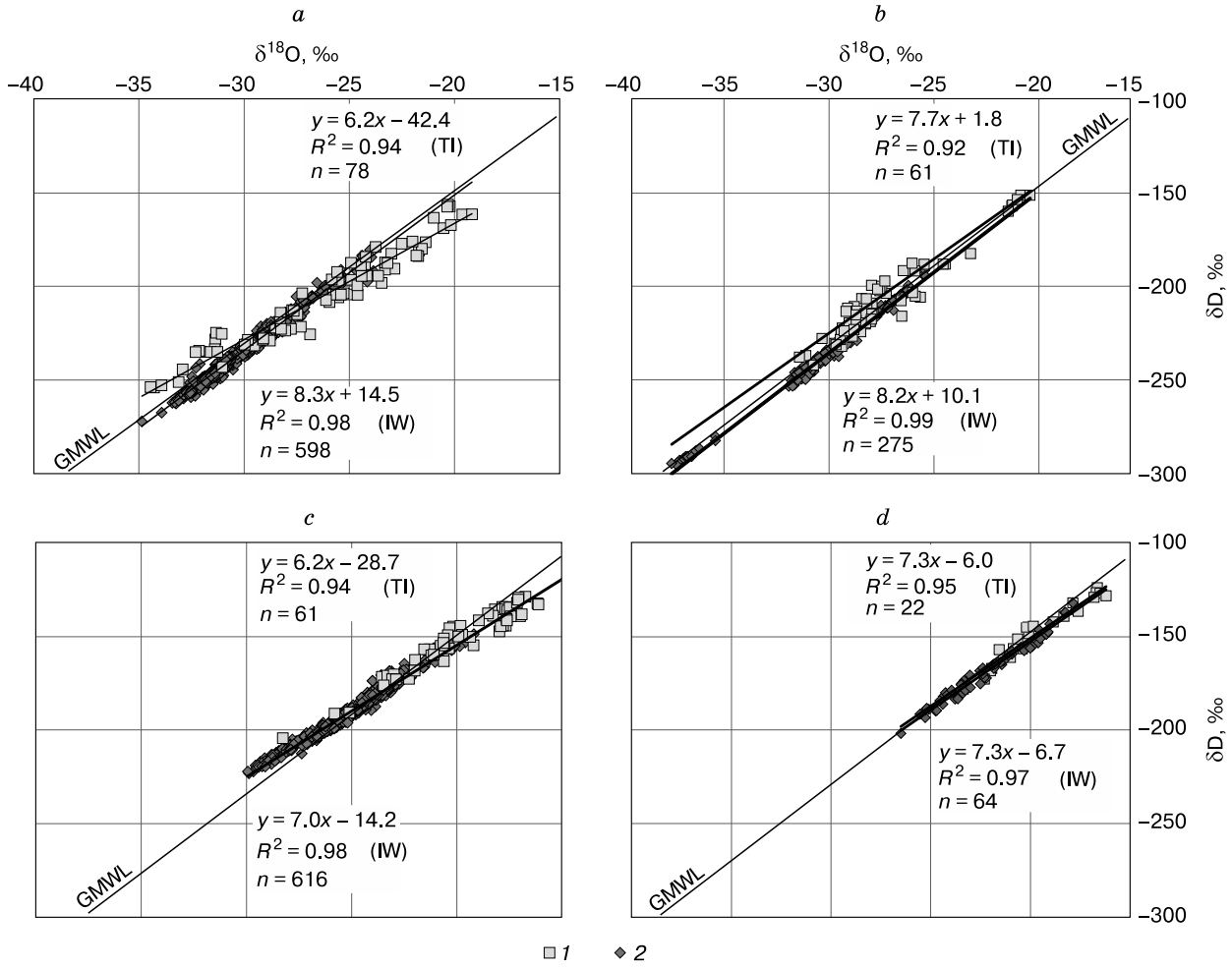

Fig. 2. $\delta^{18}O$–δD-diagrams and regression equations for texture ice and ice wedge samples:

a – Karginsky age, *b* – Sartan age, *c* – Holocene, *d* – modern (younger than 100 years). R^2 – correlation coefficient, *n* – number of samples. *1* – texture ices; *2* – ice wedges.

TI and IW samples form two "clouds", the δD–$\delta^{18}O$ ratio for which is described by linear regression equations $\delta D = a\delta^{18}O + b$ (where *a* is slope (regression) coefficient, *b* is linear intercept).

The values of *a* and *b* coefficients for TI and for IW of the considered age groups differ, and these values for Late Pleistocene and Holocene texture ices are lower than for the syngenetic ice wedges (Table 3). The low values of slope coefficient for Late Pleistocene and Holocene TI can be explained by the cryogenic and evaporation fractionation processes during their formation [*Dereviagin et al., 2013*].

A similar pattern is observed for modern precipitation: the values of the δD–$\delta^{18}O$ regression equation coefficients are lower for rainfall than for solid precipitation. According to the results of multi-year field observations in the region, the ratio *a* is equal to 7.0 for the rain, and to 7.7 for solid precipitate, while linear intercept *b* is –12.9 ‰ (rain) and 3.8 ‰ (snow), respectively. Similar results (6.9 and –15.2 ‰ for rainfall, and 7.9 and 4.8 ‰ for solid precipitation, respectively) were obtained in the course of three-year observations of the isotopic composition of precipitation at Tiksi.

Maximal differences in the slope coefficient values (*a*) for TI and IW are demonstrated in Karginsky period due to the fact that the coefficient for TI had reached a minimum value: 6.2 versus 8.3 for ice wedges. In Sartan period that succeeded it, this coefficient remained virtually unchanged for ice wedges (8.2), while for TI it grew up to 7.7 (Table 3). In the Holocene, this TI-related parameter reaches 6.2, which is equal to its value in Karginsky period.

Differences in the slope coefficient values for Karginsky, Sartan times and in the Holocene probably reflect the relationship between fractions of snowmelt and rainwater involved in the formation of texture ices; intensity of cryogenic and evaporation frac-

tionation, and are associated with highly contrasting climate in the final stages of the Pleistocene and the Holocene. Periods with very cold winters and cold dry summers, unparalleled in the Holocene, alternated with drier environments during cool summers and moderately cold winters in the Late Pleistocene [*Sher et al., 2005*]. Holocene climate was characterized by a wet and relatively warm summer (the distribution of shrub-tundra and forest-tundra) and by the winter temperature rise [*Dereviagin et al., 2010*].

A significant decrease in the regression slope coefficient for ice wedges from 8.2 to 7.0 and more than twofold increase in average d_{exc} values from 5.1 to 10.1 ‰ (Table 3) at the turn of the Late Pleistocene and Holocene may have been due to changed sources of winter precipitation [*Meyer et al., 2002b*].

Modern IW and TI are distinguished by identical slope coefficient values in the regression equation (a = 7.3), being close to the local meteoric water line slope coefficient for the region (7.6). The corresponding curves in the δD–$\delta^{18}O$-diagram run parallel to each other. The line for IW samples characteristics is located slightly above the line for TI, which is reflected in the coefficient b values (Table 3).

Determination of the deuterium excess in massive ground ice samples showed that the difference between maximum and minimum values of this parameter in texture ices significantly (1.5–2-fold) higher than that in ice wedges. For the entire collection of texture ice samples, d_{exc} values range from –10.8 to 24.2 ‰, while for ice wedges – from –4.4 to 18.0 ‰. These data underpin the inference about greater homogeneity of the isotopic composition of ice wedges compared to that of texture ices, which is associated with the peculiarities of their genesis and formation mechanism, specifically, with the influence of the isotope fractionation processes.

Variability of the isotopic composition on contacts between ice wedges and enclosing sediments

A characteristic feature of the cryogenic structure of the Ice Complex sediments consists in parallel-layered schlieren cryogenic texture, the so-called striae ("belts"), which underscore or sometimes create a layering effect on the host ice wedges [*Romanovsky and Kaplina, 1969*]. Belts are located between the ice wedges throughout the section of Ice Complex, sticking without visible contact boundary directly to ice wedges, usually creating a characteristic vertical bend near ice wedges. The configuration of segregated ice schlieren corresponds to the predated isothermal surface at the base of thaw layer in the polygons, while schlieren form as the freezing proceeds from bottom upward. The source of moisture contributing to segregated ice formation is the soil moisture within AL, which in turn is fed by meteoric waters.

Schlieren ice ("belts") thickness varies widely – from several millimeters to several centimeters. The distance between them varies from 10–20 to 30–50 cm down the section. Ice belts are generally clear, transparent, with little inclusion of air bubbles. Cryogenic texture between ice belts is massive, fine-lens-like, partly-reticulate thin-schlieren, layered thin-schlieren. Average gravimetric ice content in silty clays and silts of Ice Complex reaches 40–60 %, in the peaty varieties – in excess of 70 %.

Alas deposits are also characterized by a very high ice content (average gravimetric ice content >60–70 %) dictated by the striae and layered cryotexture. The thickness of ice schlieren reaches 2–5 cm, with spacing of 10–20 cm between them. Ice schlieren of the ice-wedge body (as well as in the sediments of Ice Complex) feature characteristic vertical bending.The side contact zones between wedge ice and the enclosing sediments often show a narrow stripe of pure and transparent ice, sometimes with a vertically oriented mineral micro-inclusions in the form of thin layers. This band termed "fringe", is associated with the processes of segregated ice formation [*Solomatin, 1965*].

The transition from milky wedge ice to the cleaner ice fringe is fuzzy, gradual. Ice fringes merge with texture-forming ice with no visible transition, the boundary between them can be traced only in the polaroid by the crystals' shape and size. The visible width of the fringe is not constant, varying from 1–3 to 5 cm. Petrographic characteristics of the side contacts of ice wedges are described in detail by *V.I. Solomatin* [*1965, 1973*].

The authors thoroughly examined and sampled ($\delta^{18}O$, δD) 82 ice wedges of the Late Pleistocene (Ice Complex) and Holocene (alas and alluvial complexes) in the Laptev Sea region during the period from 1994 to 2007. The coring of ice wedges was carried out along horizontal profiles using a specially developed methodology [*Meyer et al., 2002b; Dereviagin et al., 2010*].

Visually, the fringe which is actually a band (3–5 cm in width) of pure transparent ice on the contact between ice wedges and enclosing sediments – was observed only in 16 out of the 82 ice wedges (less than 20 %). In the overwhelming number of cases the fringe was documented in Holocene sediments in the Lena Delta (12 ice wedges) and only 4 ice wedges of Karginsky age on the Bykovsky Peninsula and Bolshoi Lyakhovsky island. In ice wedges of Sartan age, the fringe was not observed, visually. However, out of the 82 ice wedges, 54 (66 %) showed dramatic changes in the isotopic composition ($\delta^{18}O$, δD, d_{exc}) in the contact zone between ice wedges and enclosing sediments. The changes in the isotopic composition influences both ice wedges, and texture ices. In the portion of ice-wedge body nearby the side contact, a sud-

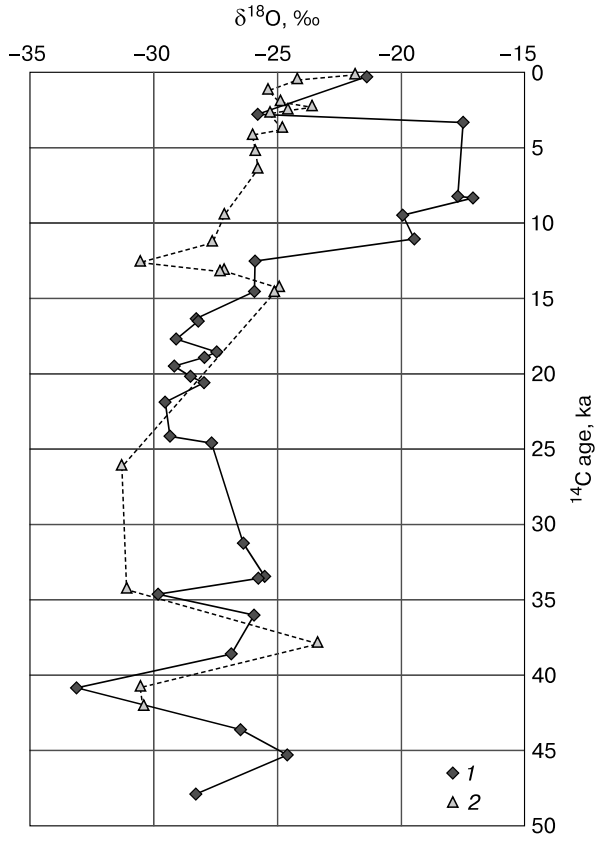

Fig. 3. Changes in oxygen-isotopic composition ($\delta^{18}O$) in Late Pleistocene (age: 50–10 ka) and Holocene ground ices according to dated (^{14}C) samples.

1 – texture ices; *2* – ice wedges.

den heavying of the isotopic composition of $\delta^{18}O$ (δD) is documented.

An increase in ^{18}O concentrations ranges from 2–3 to 5–7 ‰, with d_{exc} values thus reduced by 3–7 ‰, and in some cases by 10–12 ‰, reaching negative values. These changes are evidenced in ice wedges with width from 3–5 to 10 cm, and tend to attenuate with growing distance from the contact. Interestingly, the $\delta^{18}O$ variability may in some cases affect only one side of ice wedges, leaving the opposite side virtually unchanged. Sometimes the changes are recorded only in d_{exc} values, while $\delta^{18}O$ (δD) parameter varies insignificantly. As a result of the heavying, the isotopic composition of ice wedges are close to the isotopic composition of TI of the enclosing sediment. The opposite phenomenon is observed in ice schlieren ("belts"), welded to ice wedges: the isotopic composition becomes lighter (by 0.5–30 ‰ for $\delta^{18}O$) as it approaches ice wedges [*Dereviagin et al., 2005*] with d_{exc} values thus increasing by 0.5–2.0 ‰. These changes are documented at a distance of 0.3–0.5 m from the ice wedges.

Evidence of climate changes in the isotope composition of texture ices and ice wedges

The most spectacular changes in the isotopic composition of TI and of IW are evidenced in relation with Holocene climate warming, which is reflected similarly in the characteristics of the isotopic composition of both texture ices, and ice wedges (Tables 2, 3): Holocene ices became generally heavier ($\delta^{18}O$ values) by 7.5 ‰ for texture ices and by 5.1 ‰ for ice wedges. At the same time, average values of deuterium excess in TI decreased by 3.6 ‰, and by 5 ‰ in ice wedges. While parameters of the δD–$\delta^{18}O$ regression equation demonstrated significant transformations: for both types of ice, the value of regression slope and intercept have decreased.

In the course of research, radiocarbon dating was applied to 30 TI samples and 23 IW samples to determine their ages (Table 1). ^{14}C-dating of oldest samples were found to be 47.9 ka (TI) and 42.0 ka (IW). Fig. 3 showing plots derived from the data on isotopic composition ($\delta^{18}O$) of dated TI and IW samples allows to observe changes in isotopic oxygen composition of Late Pleistocene (50–10 ka) and Holocene ground ices.The oldest stage (older than 34 ka) is characterized by violent saw-tooth-like oscillations of $\delta^{18}O$ values for TI with peaks at –33.1 ‰ (40.8 kya) and –24.6 ‰ (45.3 kya). At this, $\delta^{18}O$ values for ice wedges largely replicate the diagram trajectory for TI, remaining slightly heavier (by 1–2 ‰) at some sites. The presence of "warm" anomaly in $\delta^{18}O$ of ice wedges from –23.4 ‰ (ca. 38 kya) are corroborated by increased $\delta^{18}O$ of TI from –33.1 ‰ (40.8 kya) to –25.9 ‰ (38.6 kya) and –25.1 ‰ (36.0 kya). The featuring geological section of deposits formed in the period of 45–35 kya, which include numerous lenses and layers of peat is of particular interest [*Schirrmeister et al., 2011*]. This suggests more dynamic actions of climate and landscapes.

In the interval of 34–25 kya the $\delta^{18}O$ values for IW and TI are stable and range from –30 to –31 and from –25.5 to –27.7 ‰, respectively. In the period to follow (24–16 kya), these indicators for $\delta^{18}O$ persist with small oscillations at a very low level and are stable (–28.0...–29.5 ‰) in texture ices. In the interval of 34–15 kya there are only three dated ice cores from ice wedges, though, which means that any correct interpretation of the available data would be problematic.

Late Sartan–Early Holocene period is marked by a rapid growth of $\delta^{18}O$ in TI from –29.1 to –28.2 ‰ (17.7–16.5 kya) to –19.5 ‰ (11.1 kya). The increasing trend towards extremely high $\delta^{18}O$ values remained until as late as 8.3–8.2 ka (–17.7...–17.1 ‰). Most likely, the marked increase in $\delta^{18}O$ of TI was associated with global warming, responsible for changes (weighting) in the isotopic composition of precipitation.

The first dated samples of ice wedges associated with early Holocene warming (14.2; 14.5 kya), with $\delta^{18}O$ values equal –24.9 and –25.1 ‰, which is about 5 ‰ heavier than the average for Sartan period. Climate cooling, corresponding to different stages of Dryas, is clearly documented in IW samples (13.1–11.2 kya) with the minimum at –30.5 ‰ (12.5 kya), indicating a significant decrease in the mean winter air temperature during this period. The reliability of these data is corroborated by detailed studies of the isotopic composition of ice wedges, dated as Younger Dryas in the Canadian Arctic [*Meyer et al., 2010*]. It should be emphasized that the available data show no decrease in $\delta^{18}O$ of TI during Young Dryas. Unfortunately, the amount of ice cores is not sufficient for any valid conclusions [*Meyer et al., 2015*].

The isotopic composition of Holocene ice wedges is represented by a series of 12 samples with ages dated in the range from 9.3 kya to contemporary time (<100 years). The samples from this range exhibit a stable trend for the isotopic composition weighting ($\delta^{18}O$) from –27.1 to –21.9 ‰. It is 3–8 ‰ higher than those for the preceding cold period, correlated with Dryas (–30.5 ‰). Fluctuations of $\delta^{18}O$ in ice wedges reflect the general trend for climate warming during winter in the region, with its progression into the present time [*Meyer et al., 2015*].

Beginning from late Sartan time (11.1 kya) and until late Holocene, the $\delta^{18}O$ values for texture ices increased from –19.9 ‰ (9.5 kya) to –17.5 ‰ (3.3 kya). During the following period (3.3–2.8 kya), the isotopic composition suddenly became lighter (to –25.8 ‰), which was succeeded by its heavying to –21.4 ‰. Contemporary average $\delta^{18}O$ values for texture ices and ice wedges amount to –19.9 and –22.2 ‰, respectively. The $\delta^{18}O$ value (–21.9 ‰) for one of the youngest dated sample from ice wedges (<100 years) is close to the youngest dated sample from texture ices (300 years) and equals –21.4 ‰.

The isotopic record derived from dated samples of ground ices has huge gaps for thus far missing data. In addition, climatic signal can be largely distorted by the influences from other factors. This essentially complicates the interpretation of paleoclimatic data on changes in the isotopic composition of ground ices. A further development of this promising research line is associated with obtaining new data, to fill in the existing gaps.

CONCLUSIONS

1. The research results demonstrated significant differences in the characteristics of the isotopic composition of texture ices and ice wedges at the Laptev Sea coast:

– TI have proven isotopically heavier than ice wedges on average by 4.2 ‰ for Karginsky, by 3.0 ‰ for Sartan, and by 5.4 ‰ for Holocene ices;

– variability (range of values) of the isotopic composition ($\delta^{18}O$, δD and d_{exc}) characteristics is greater for texture ices versus ice wedges;

– the value of the slope coefficient (a) in the δD–$\delta^{18}O$ regression equation for the Late Pleistocene texture ices is lower than for ice wedges of the same age; in the Holocene, this difference reduces, while slope coefficients are equal for modern texture ices and ice wedges.

2. The revealed differences in the isotopic characteristics of texture ices and ice wedges are determined by the peculiarities of their genesis and mechanisms of formation. One of the main genetic factor is the relationship between snowmelt and rainwater in the formation of ice. In addition, the isotopic characteristics of texture ices may have a significant impact on isotopic fractionation processes and the composition of the enclosing sediments (presence of peat).

3. In the contact zone between ice wedges and texture ices, there was observed a change in their isotopic composition, indicating the mass transfer between them during their formation. The width of this zone in ice wedges is up to 10 cm, up to 50 cm in the enclosing sediment (TI), and it includes fragments of ice wedges on the side contacts with a modified structure (“fringe”) and parts of ice schlieren (“belts”) in the enclosing sediments containing ice wedges.

4. Global warming at the end of the Late Pleistocene resulted in the increases average $\delta^{18}O$ values by 7.5 ‰ for texture ices and by 5.1 ‰ for ice wedges. The isotope shift being that large in texture ices, it probably is responsible for an increase in summer temperatures and rainfall. Recent warming (in the past 100 years) generally featured by warmer winters has affected only the isotopic composition of ice wedges, while average $\delta^{18}O$ and δD values for texture ices tend to differ little from the oldest Holocene formations.

5. Time series analysis for $\delta^{18}O$ values by ^{14}C-dated samples of texture ices and ice wedges shows that, while reflecting large-scale climate changes over the past 40–45 thousand years they react in a similar way to them. At the same time, the response of the isotopic composition of texture ices and ice wedges to the paleoclimatic events may vary, which is associated with the nature of their genesis. The contribution of isotopic analysis of the dated samples from ice wedges and texture ices to the wealth of data will benefit reconstructions of climate change and its prediction.

References

Andreev, A.A., Schirrmeister, L., Siegert, Ch., et al., 2002. Paleoenvironmental changes in northeastern Siberia during the Late Quaternary – evidence from pollen records of the Bykovsky Peninsula. Polarforschung, vol. 70, 13–27.

Dansgaard, W., 1964. Stable isotopes in precipitation. Tellus, vol. 16, 436–468.

Dereviagin, A.Yu., Chizhov, A.B., Meyer, H., 2010. Winter temperature conditions in the Laptev Sea region during the last 50 thousand years in the isotopic record ice-wedges record. Kriosfera Zemli XIV (1), 32–40.

Dereviagin, A.Yu., Chizhov, A.B., Meyer, H., 2011. Most recent climate changes according to the isotopic composition of ground ice, in: Proceed. of IVth Conference of Russian geocryologists. Univer. kniga, Moscow, vol. 2, pp. 47–52. (in Russian)

Dereviagin, A.Yu., Chizhov, A.B., Mayer, H., Opel, T., Schirrmeister, L., Wetterich, S., 2013. Isotopic composition of texture ice at the Laptev Sea coast. Kriosfera Zemli XVII (3), 27–34.

Dereviagin, A.Yu., Chizhov, A.B., Mayer, H., Syromiatnikov, I.I., 2005. Isotopic composition of segregated ice of the Ice Complex at the Bykovsky Peninsula, in: Proceed. of IIIrd Conference of Russian Geocryologists. Moscow Univ. Press, Moscow, vol. 1, pp. 162–168. (in Russian)

Mackay, J.R., 1983. Oxygen isotope variations in Permafrost, Tuktoyaktuk Peninsula area, Northwest Territories. Current Res., Pt B, Geol. Surv. Can., Pap. 83-1B, pp. 67–74.

Meyer, H., Dereviagin, A.Yu., Siegert, Ch., Hubberten, H.-W., 2002a. Hydrogen and oxygen isotopes in ground ice – A valuable tool for paleoclimatic studies on Big Lyakhovsky Island, North Siberia. Permafrost and Periglacial Processes, vol. 13, 91–105.

Meyer, H., Dereviagin, A.Yu., Siegert, Ch., Hubberten, H.-W., 2002b. Paleoclimate studies on Bykovsky Peninsula, North Siberia – hydrogen and oxygen isotopes in ground ice. Polarforschung, vol. 70, 37–51.

Meyer, H., Opel, T., Laepple, T., Dereviagin, A.Yu., Werner, M., Hoffmann, K., 2015. Long-term winter warming trend in the Siberian Arctic during the mid to late Holocene. Nature Geoscience, 8 (2), 122–125, doi: 10.1038/ngeo2349.

Meyer, H., Schirrmeister L., Yoshikawa, K., et al., 2010. Permafrost evidence for severe winter cooling during the Younger Dryas in northern Alaska. Geophys. Res. Lett., vol. 37, L03501, doi: 10.1029/2009GL041013.

Opel, T., Dereviagin, A.Yu., Meyer, H., Wetterich, S., 2011. Paleoclimatic information from stable water isotopes of Holocene and recent ice wedges at the Oyogoss Yar coast region (Northeastern Siberia). Permafrost and Periglacial Processes, vol. 24, 84–100, doi: 10.1002/ppp.667.

Romanovsky, N.N., Kaplina, T.N., 1969. Types of layers bending in ice wedge polygons, in: Merzlotnye issledovania. Moscow Univ. Press, Moscow, iss. IX, pp. 57–68. (in Russian)

Schirrmeister, L., Grosse, G., Kunitsky, V., et al., 2008. Periglacial landscape evolution and environmental changes of Arctic lowland areas for the last 60 000 years (Western Laptev Sea coast, Cape Mamontov Klyk). Polar Res. 27 (2), 249–272.

Schirrmeister, L., Kunitsky, V.V., Grosse, G., Wetterich, S., Meyer, H., Schwamborn, G., Babiy, O., Derevyagin, A.Yu., Siegert Ch., 2011. Sedimentary characteristics and origin of the Late Pleistocene Ice Complex on North-East Siberian Arctic coastal lowlands and islands – a review. Quatern. Intern., vol. 241, iss. 1–2, pp. 3–25.

Sher, A.V., Kuzmina, S.A., Kuznetsova, T.V., Sulerzhitsky, L.D., 2005. New insights into the Weichselian environment and climate of the East Siberian Arctic, derived from fossil insects, plants, and mammals. Quatern. Sci. Rev., vol. 24, 533–569.

Solomatin, V.I., 1965. On structure of ice-wedges, in: Podzemnyi Lyod. Moscow Univ. Press, Moscow, iss. II, pp. 46–73. (in Russian)

Solomatin, V.I., 1973. Segregation processes on the side contacts of ice wedges, in: Problemy Kriolotologii. Moscow Univ. Press, Moscow, iss. 3, pp. 183–192. (in Russian)

Vaikmae, R., 1989. Oxygen isotopes in permafrost and ground ice – a new tool for paleoclimatic investigations, in: Proc. of the 5th Working Meeting "Isotopes in Nature". Leipzig, DDR, pp. 543–553.

Vasil'chuk, Yu.K., 1992. Oxygen-isotope composition of ground ice (application to paleogeocryological reconstructions). Izd. OTP RAN; MGU; PNIIS, Moscow, vol. 1, 420 pp.; vol. 2, 264 pp. (in Russian)

Wetterich, S., Rudaya, N., Tumskoy, V., et al., 2011. Last Glacial Maximum records in permafrost of the East Siberian Arctic. Quatern. Sci. Rev., vol. 30, 3139–3151.

Yershov, E.D. (Ed.), 1989. Geocryology of the USSR. Central Siberia. Nedra, Moscow, 414 pp. (in Russian)

Received December 25, 2014